




The transcriptional regulator Sin3A balances IL-17A and Foxp3 expression in primary CD4 T cells

Laura Perucho¹, Laura Icardi¹, Elisabetta Di Simone¹, Veronica Basso¹, Alessandra Agresti¹ , Amaia Vilas Zornoza^{2,3}, Teresa Lozano⁴, Felipe Prosper^{2,3}, Juan José Lasarte⁴  & Anna Mondino^{1,*} 

Abstract

The Sin3 transcriptional regulator homolog A (Sin3A) is the core member of a multiprotein chromatin-modifying complex. Its inactivation at the CD4/CD8 double-negative stage halts further thymocyte development. Among various functions, Sin3A regulates STAT3 transcriptional activity, central to the differentiation of Th17 cells active in inflammatory disorders and opportunistic infections. To further investigate the consequences of conditional Sin3A inactivation in more mature precursors and post-thymic T cell, we have generated CD4-Cre and CD4-CreER^{T2} Sin3A^{F/F} mice. Sin3A inactivation *in vivo* hinders both thymocyte development and peripheral T-cell survival. *In vitro*, in Th17 skewing conditions, Sin3A-deficient cells proliferate and acquire memory markers and yet fail to properly upregulate *Il17a*, *Il23r*, and *Il22*. Instead, IL-2⁺ and FOXP3⁺ are mostly enriched for, and their inhibition partially rescues IL-17A⁺ T cells. Notably, Sin3A deletion also causes an enrichment of genes implicated in the mTORC1 signaling pathway, overt STAT3 activation, and aberrant cytoplasmic RORγt accumulation. Thus, together our data unveil a previously unappreciated role for Sin3A in shaping critical signaling events central to the acquisition of immunoregulatory T-cell phenotypes.

Keywords FoxP3; IL-17A; RORγt; Sin3A; T lymphocytes

Subject Categories Chromatin, Transcription & Genomics; Immunology; Signal Transduction

DOI 10.15252/embr.202255326 | Received 29 April 2022 | Revised 12 February 2023 | Accepted 17 February 2023 | Published online 16 March 2023

EMBO Reports (2023) 24: e55326

Introduction

The Sin3 transcriptional regulator homolog A (Sin3A) is the core component of a multiprotein chromatin-modifying complex. While initially defined as a co-repressor, Sin3A is now considered a co-regulator, since it has co-repressor, co-activator, and transcription factor properties (Chaubal & Pile, 2018). Sin3A contains four paired amphipathic helix domains (Ayer *et al*, 1995; Schreiber-Agus

et al, 1995), each of them specific for particular transcriptional regulators. Through a class I histone deacetylases (HDAC) interaction domain (HID), Sin3A binds HDAC1 and HDAC2 and influences chromatin structures (Alland *et al*, 1997; Laherty *et al*, 1997; Nagy *et al*, 1997). Sin3A-associated HDAC1/2-activity is essential for embryonic stem cell survival (Fazzio *et al*, 2008), hematopoiesis, hematopoietic stem cell homeostasis, and T and B lymphocyte development (Heideman *et al*, 2014). While HDAC activities are regarded as predominant, other chromatin modifiers were also found in Sin3A complexes, including histone methyltransferases (Nakamura *et al*, 2002), O-linked N-acetylglucosamine transferase (Yang *et al*, 2002), or members of the Swi/Snf nucleosome remodeling complex (Pal *et al*, 2003).

Sin3A deletion caused the deregulation of genes involved in cell cycle, DNA replication, DNA repair, apoptosis, chromatin modification, mitochondrial metabolism and cell differentiation *in vitro* (Dannenber *et al*, 2005), and early embryonic lethality (Cowley *et al*, 2005; Dannenberg *et al*, 2005; McDonel *et al*, 2012). Its conditional inactivation at the double-negative (DN) stage of thymocyte development was found to cause a reduction in cellularity accompanied by an arrest in CD8 T-cell selection and the appearance of dysfunctional CD4⁺ T cells (Cowley *et al*, 2005).

In previous studies, Sin3A was shown to regulate the transcriptional activity of the signal transducer and activator of transcription 3 (STAT3) (Icardi *et al*, 2012; Gambi *et al*, 2019), which is central to differentiation of Th17 cells. These cells mediate immunity against fungal infections and extracellular bacteria (Ye *et al*, 2001) through the secretion of several proinflammatory cytokines including IL-17A, IL-17F, IL-21, IL-22, IL-9, GM-CSF, TNFα, and CCL20 (Liang *et al*, 2006; Dong, 2008). Complex signaling networks shape differentiation of Th17 cells (Yosef *et al*, 2013). Signals originated through the T-cell receptor (TCR) and co-stimulatory molecules, such as CD28, in the presence of IL-6 (Das *et al*, 2009) activate a number of transcription factors, among which is STAT3, which is required during early Th17 cell differentiation (Mathur *et al*, 2007; Yang *et al*, 2007; Zhou *et al*, 2007). STAT3, in turn, controls the expression of the retinoic-acid-receptor-related orphan receptor-γ (RORγt), the lineage-specific transcriptional regulator of Th17 (Ivanov *et al*, 2006). IL-6 and TGF-β also cause the STAT3-dependent

1 Lymphocyte Activation Unit, Division of Immunology, Transplantation and Infectious Diseases, IRCCS San Raffaele Scientific Institute, Milan, Italy

2 Departamento de Hematología, Clínica Universidad de Navarra and CCUN, IDISNA, Universidad de Navarra, Pamplona, Spain

3 Centro de Investigación Biomédica en Red de Cáncer (CIBERONC), Pamplona, Spain

4 Immunology and Immunotherapy Program, Center for Applied Medical Research (CIMA), CCUN, IDISNA, University of Navarra, Pamplona, Spain

*Corresponding author. Tel: +390226434801; E-mail: anna.mondino@hsr.it

expression of IL-21, which act via an autocrine loop to promote ROR γ t-dependent IL-17 expression (Korn *et al*, 2007, 2009; Wei *et al*, 2007). Transcription cofactors have also been shown to regulate Th17 cell development (Jiang *et al*, 2019). In addition to act on gene transcription, STAT3 has been shown to control mitochondrial Ca $^{2+}$ and membrane potential, contributing to CD4 $^{+}$ T-cell differentiation (Yang *et al*, 2015; Rincon & Pereira, 2018).

Given the role of STAT3 in Th17 cell differentiation, and the finding that Sin3A controls STAT3 in other cell types (Icardi *et al*, 2012; Gambi *et al*, 2019), we hypothesized that Sin3A could contribute to CD4 $^{+}$ T-cell differentiation. To define the role of Sin3A and understand the consequences of its inactivation in CD4 cells in mature T cells, we crossed Sin3A $^{F/F}$ mice with CD4-Cre, CD4-CreER T2 , and Rosa26-CreER T2 deleter strains, in the hope that allowing the deletion of Sin3A *in vivo* past the DN stage would promote proper development of mature T cells. We found that the deletion of Sin3A in DP precursor or mature T cell *in vivo* hindered T-cell survival. By contrast, deleting Sin3A *in vitro* in mature T cells allowed proliferation and acquisition of memory markers. We provide evidence supporting the role for Sin3A in fine tuning IL-2, mTOR, STAT3, and ROR γ t-dependent events over the course of Th17 differentiation, ultimately balancing IL-17A and Foxp3 expression and shaping Th17 cell effector functions.

Results

CD4-Cre-driven Sin3A inactivation halts proper thymocyte development

A previous report found that Sin3A deletion in DN thymocytes via Lck-driven Cre expression hindered CD8 thymocyte development and caused post-thymic accumulation of dysfunctional CD4 $^{+}$ T cells (Cowley *et al*, 2005). To further investigate the contribution of Sin3A to mature CD4 $^{+}$ T differentiation, we crossed Sin3A $^{F/F}$ with CD4-Cre mice (Sin3A-CD4 Δ) and CD4-CreER T2 deleter strains. We hypothesized that Sin3A inactivation beyond the DN stage of thymocyte development (i.e., past the pre-TCR assembly and over the course of DP to SP transition) would be permissive for further thymic maturation. We first analyzed the phenotype of CD4-Cre mice. Flow cytometry (FACS) analyses revealed that both CD4SP and CD8SP cells were significantly underrepresented in Sin3A-CD4 Δ mice when compared to controls (Fig 1A and B). This correlated with Sin3A expression, comparable in DN cells and, respectively, reduced and completely lost in DP and SP cells derived from Sin3A-CD4 Δ mice compared with controls (Fig 1C). Although thymus cellularity was not different (Appendix Fig S1A), total numbers of CD4SP and CD8SP cells were significantly reduced in Sin3A-CD4 Δ mice when compared to controls (Appendix Fig S1B). Among these, also CD4 $^{+}$ Foxp3 $^{+}$ cells were reduced (Appendix Fig S1C). Reduced frequencies and total number reflected increased apoptotic cell death during positive selection (Appendix Fig S1D and E). Thus, in line with the previous report by Cowley *et al* (2005), deleting Sin3A in thymocyte precursors severely hinders cell survival and further maturation. Impaired thymic development was reflected by the severe reduction in the frequency of CD4 $^{+}$ and CD8 $^{+}$ T cells in secondary lymphoid organs (Fig 1D and E). Of note, remaining CD4 $^{+}$ T cells in the spleen of Sin3A-CD4 Δ mice had acquired a CD44 high

CD62L low effector memory phenotype (Fig 1F–H). This was likely the results of cells having escaped CD4-Cre-driven Sin3A deletion (Fig 1H), and having acquired a memory phenotype as a result of lymphopenia induced proliferation (Sckisel *et al*, 2017). We also looked for possible differences in CD4 $^{+}$ CD25 $^{+}$ FoxP3 $^{+}$ cells. Data depicted in Appendix Fig S2 confirm lower frequency of CD4 T cells in the blood of Sin3A-CD4 Δ mice (Appendix Fig S2A). Given selective enrichment of CD4 T cells escaping deletion, and of T cells with CD44 high CD62L low effector memory phenotype, we gated the cells according to naive/memory phenotype and Sin3A levels (Sin3A-CD4 Δ mice) (Appendix Fig S2B). Data indicate comparable percentages of CD4 $^{+}$ CD25 $^{+}$ FoxP3 $^{+}$ cells (Appendix Fig S2C). Thus, overall Sin3A inactivation at the DP stage of thymocyte development hinders proper representation of mature CD4 $^{+}$ T cells.

We then attempted conditional deletion via tamoxifen administration to Sin3A $^{F/F}$ CD4-CreER T2 mice. Tamoxifen administration caused a progressive loss of circulating mature CD4 $^{+}$ T cells (Appendix Fig S3A and B). Thus, conditional deletion of Sin3A in DN (Cowley *et al*, 2005) or DP (Fig 1 and Appendix Figs S1–S3) precursors unequivocally defines a role for Sin3A in thymocyte development and underlines the need for post-thymic inactivation for the analysis in mature T cells.

Sin3A deletion in mature CD4 T cells imprints a mTORC1 signature and hinders Th17 cell differentiation

To investigate the impact of Sin3A deletion in mature T cells, CD45.2 CD4-CreER $^{T2-/-}$ Sin3A F/F and CD4-CreER $^{T2+/-}$ Sin3A F/F mice were treated with tamoxifen for 4 days. This is sufficient to reduce Sin3A levels in peripheral T cells. T cells were then recovered, mixed with equal numbers of CD45.1 congenic T cells, and transferred in NSG recipients (a schematic representation of the experiment is depicted in Appendix Fig S3C). T-cell persistence was then monitored by FACS analysis. Data depicted in Appendix Fig S3D indicate that compared with Sin3A-sufficient cells, Sin3A-deficient cells persisted to lower extents. Of note, by Day 20, remaining T cells within the CD4-CreER $^{T2+/-}$ Sin3A $^{F/F}$ mice expressed Sin3A to normal levels suggestive of preferential survival of cells that escaped deletion. Thus, mature T cells need Sin3A for *in vivo* survival, even at the post-thymic stage of development, hindering the characterization of Sin3A to mature T-cell differentiation *in vivo*.

We thus resorted to *in vitro* analysis. We first investigated Sin3A expression in purified CD4 $^{+}$ T cells and found it to be upregulated by Day 3 of anti-CD3/CD28 activation in various skewing condition (Fig 2A) and over the course of Th17 differentiation (Fig 2B). Next, we cultured purified CD4 $^{+}$ T cells obtained from CD4-Cre CreER $^{T2+/-}$ Sin3A $^{F/F}$ or Rosa26-CreER $^{T2+/-}$ Sin3A $^{F/F}$ mice for 6 days in interleukin 7 (IL-7) in the absence or the presence of 4-hydroxytamoxifen (TAM). This was adopted to allow Cre-mediated Sin3A deletion in mature T cells while avoiding activation (Tan *et al*, 2001). To investigate the contribution of Sin3A to Th17 differentiation, cells were then cultured for an additional 3 days in Th17 skewing conditions (refer to Fig 2C for a schematic experimental outline). Western blot and FACS analysis depicted in Fig 2 report the loss of Sin3A expression in TAM-treated cells derived from Rosa26-CreER $^{T2+/-}$ Sin3A $^{F/F}$ mice (Fig 2D and E), which were then adopted for all further studies.

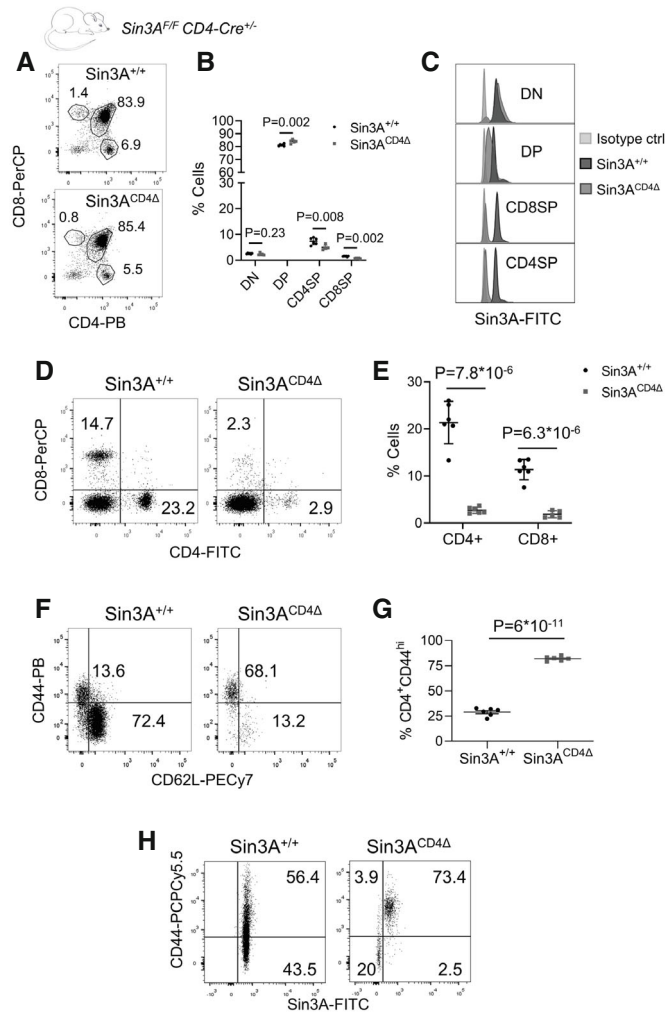


Figure 1. CD4-cre-driven Sin3A deletion halts further CD4 and CD8 thymocyte development.

A, B Representative flow cytometry analysis of CD4⁺ and CD8⁺ thymocytes (A), and frequencies of DN, DP and SP cells in Sin3A^{+/+} and Sin3A^{CD4Δ} mice (B). N = 5.
 C Sin3A intracellular levels in DN, DP, CD8SP, and CD4SP cells from Sin3A^{+/+} and Sin3A^{CD4Δ} mice.
 D, E Representative FACS of splenic CD4⁺ and CD8⁺ cells (D) and frequencies (E). N = 6.
 F, G Representative dot plots of CD44 and CD62L levels of gated CD4⁺ viable T cells (F) and quantification (G). N = 6.
 H Representative dot plots of CD44 and Sin3A levels in Sin3A^{+/+} and Sin3A^{CD4Δ} CD4⁺ T cells.

Data information: In (B, E, G), data are presented as mean (Bars) ± SD. Two-tailed unpaired Student's t-test. Dots depict individual mice analyzed in independent experiments.

Over the course of Th17 skewing, both control and TAM-treated cells completed several rounds of cell division, indicated by the dilution of the Tag-IT violet vital dye (Fig 3A and B). Fewer TAM-treated cells completed more than three cell division cycles (Fig 3B). This was paralleled by lower cellular yields (Fig 3C), and a slightly increase in apoptotic cells (Appendix Fig S4A and B), and in cells in the S phase of the cell cycle (Appendix Fig S4C). To some extent,

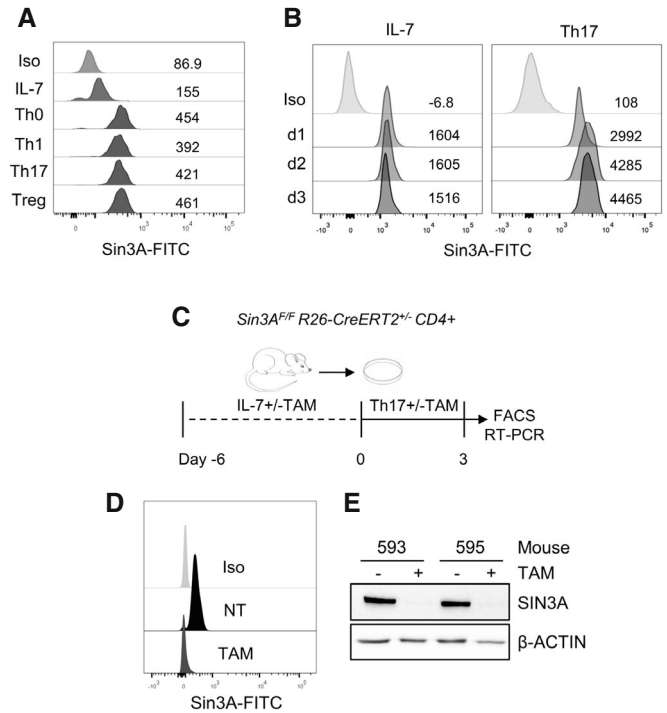


Figure 2. Sin3A levels are increased over the course of activation and differentiation.

A Representative flow cytometric analysis of Sin3A expression in wild-type CD4⁺ T cells kept for 3 days in IL-7 or differentiated to Th0, Th1, Th17 and Treg.
 B Kinetics of Sin3A upregulation in Th17 conditions.
 C Graphic representation of *ex-vivo* deletion of Sin3A. CD4⁺ T cells were purified from secondary lymphoid organs derived from Sin3A^{F/F} Rosa26-CreERT2^{+/−} mice, and kept in IL-7 for 6 days in the absence or the presence of 4-hydroxy tamoxifen (TAM). Cells were then harvested and cultured for an additional 3 days in Th17 skewing conditions in the absence or the presence of TAM.
 D, E (D) Flow cytometric and (E) Western blot analyses of Sin3A levels. Data are also depicted in Fig S5B as part of the same source file.

Source data are available online for this figure.

this recapitulates the phenotype of mouse embryonic fibroblasts, embryonic stem cells (Fazzio *et al*, 2008) and pluripotent cells (Dannenberg *et al*, 2005), and defective survival observed upon Sin3A inactivation in thymocyte precursors (Fig 1 and Cowley *et al*, 2005).

Over the course of proliferation in Th17 skewing conditions Sin3A-deficient cells acquired memory markers. Indeed, while IL-7-cultured CD4⁺ T cells retained a CD44^{low}, CD62L^{high} naïve phenotype, and lacked expression of activation markers such as CD25, PD-1, or CD69 (Appendix Fig S5A), most of Sin3A-sufficient and -deficient Th17-skewed T cells acquired a CD44^{high}, CD62L^{low} effector memory phenotype (Fig 3D and E), and upregulated CD69, CD25, PD-1 (Appendix Fig S5B and C).

To investigate T-cell behavior in response to a nominal antigen, we generated ovalbumin-specific TCR transgenic OTII^{+/−} Sin3A^{F/F} CreERT2^{+/−} mice. CD4 T cells purified from these mice were then compared to those derived from OTII^{+/−} Sin3A^{+/F} CreERT2^{+/−} littermates to also control for Cre-mediated toxicity (Loonstra

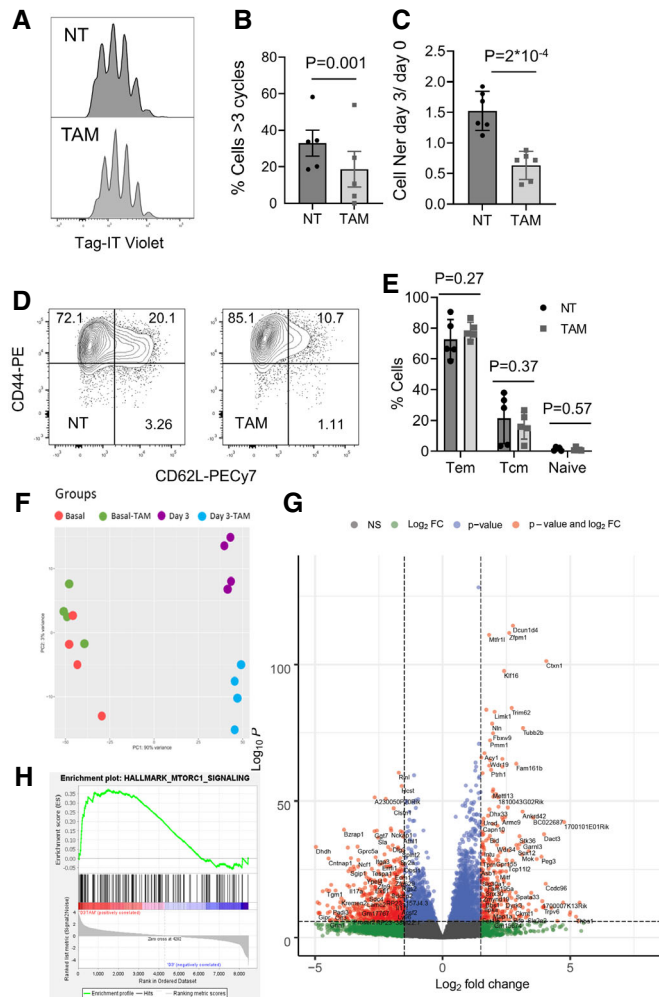


Figure 3. Conditional deletion of Sin3A allows cell differentiation and imprints T cells with a mTORC1 signature.

Sin3A^{F/F} Rosa26-CreER^{T2} CD4⁺ T cells were treated as described in Fig 2C.

- A Proliferation profiles of untreated (NT) and TAM-treated (TAM) cells labeled with Tag-IT Violet, and kept for 3 days in Th17 conditions.
- B Quantification of cell division cycle according to Tag-IT Violet dilution profiles, $N = 5$.
- C Relative cell numbers (Day 3/Day 0), $N = 6$.
- D Contour plots depicting relative CD44 and CD62L expression after gating on viable lymphocytes.
- E Bar plots showing relative frequencies of effector memory (Tem), central memory (Tcm) and naïve cells viable lymphocytes, $N = 5$.
- F–H RNA-seq transcriptomic analysis of CD4⁺ T cells derived from Rosa26-CreER^{T2} Sin3A^{F/F} mice cultured for 3 days in IL-7 in the absence or the presence of tamoxifen (basal, basal TAM) and then cultured for three additional days in Th17 polarizing conditions (Day3 or Day3TAM). Principal component analyses (F). Volcano plot of differentially expressed genes (FDR < 0.05; vertical dashed lines indicate fold change values Long2 fold change 1-1) (G) Gene Set Enrichment analysis (H) highlights a signature compatible with an mTORC1 signaling pathway (Genes up-regulated through activation of mTORC1 complex).

Data information: (A, D) Flow cytometric analyses. In (B, C, E) data are presented as mean (Bars) \pm SD. Two-tailed paired Student's *t*-test. $N = 5$ cultures per condition (NT or TAM) derived from individual mice. In (F–H) RNA Seq Omnibus GSE196615 (<https://www.ncbi.nlm.nih.gov/geo/query/acc.cgi?acc=GSE196615>).

et al, 2001). CD4 T cells were purified and treated or not with TAM, labeled with Tag-IT violet and then stimulated with the ovalbumin-derived peptide OVA₃₂₃₋₃₃₉. Data depicted in Appendix Fig S6A and B indicate that stimulating the cells with the OVA₃₂₃₋₃₃₉ peptide induced proliferation of both Sin3A-sufficient and -deficient cells. Despite OTII cells lacking Sin3A (OTII^{+/-} Sin3A^{+/-} CreERT2^{+/-}) revealed a mild proliferative and survival defect compared with controls, they similarly acquired a CD44^{high}, CD25^{high} phenotype (Appendix Fig S6C). Thus, together these data indicate that deletion of Sin3A in mature T cells is compatible with TCR-driven proliferation and differentiation into memory cells.

To obtain an unbiased overview of the impact of Sin3A inactivation on Th17 differentiation, we next performed RNA-seq analysis. To this aim, highly purified CD4⁺ T cells were kept for 6 days in IL-7 without or with TAM (Basal or BasalTAM), and then cultured for 3 additional days in Th17 polarizing conditions (Day3 or Day3TAM). RNA was then isolated and sequenced for transcripts differential expression. Most of the transcript variation segregated CD4⁺ T cells by the Th17 polarizing conditions. First principal components (PC1) analyses accounted for 90% of the variance between Th17 polarized T cells and unstimulated cells (basal conditions), and clearly differentiated Day3 samples (Sin3A sufficient) from Day3TAM ones (Sin3A deficient) (Fig 3F). Comparison between Day3TAM and Day3 T cells yielded a total of 9,386 differentially expressed genes ($P < 0.05$). Among them, 1,139 genes were upregulated and 2,282 were downregulated in Day3TAM T cells compared with controls ($P < 0.05$), when considering genes with a fold change > 1, as represented in the Volcano plot (Fig 3G). Gene set enrichment analysis (GSEA) was next performed comparing Day3TAM and Day3 samples. We found a significant enrichment of genes implicated in mTORC1 signaling pathway (Genes upregulated through activation of mTORC1 complex) (Fig 3H, Nominal P -value < 0.001, FDR q -value: 0.147). The heatmap of the top 35 up- and downregulated genes among the 181 of the mTORC1 signature is depicted in Appendix Fig S7A. As mTORC1 controls both STAT3 phosphorylation, and Th17 differentiation (Nagai *et al*, 2013), the finding that genes implicated in mTORC signaling are enriched upon Sin3A inactivation, supports its role in Th17 differentiation.

In trying to deepen the analysis, we chose to adopt a different approach. We considered only those genes that were upregulated ($5 > \log_2FC > 1$) or only downregulated ($-1 > \log_2FC > -7$) with an adjusted P -value < 0.01 to generate gene lists to be compared with available data bases by the EnrichR engine. When using the downregulated ones, we found them to belong to the cytokine receptor interaction (adj P -value < 0.002) and IL-17 signaling pathway (adj P -value < 0.02). When using the upregulated ones, we found them to belong to amino acid, vitamin, and fatty acid metabolism ($0.001 < P$ -value < 0.05) (Appendix Fig S7B and C). These additional computational analyses were in line with the enrichment of genes implicated in mTORC signaling and the role of Sin3A in shaping Th17 cells.

Finally, to even more directly analyze Sin3A-dependent transcriptional regulation, we possible overlaps of the identified gene lists with the ENCODE (transcription) plus ChEA (Chip-ex) integrated database (Lachmann *et al*, 2010). We found that downregulated genes overlapped with the Polycomb 2-regulated gene group,

while the upregulated ones overlapped with gene groups controlled by *myc*/*max* family members (Appendix Fig S7D and E). These further analyses suggest that Sin3A may play a broader than expected role in T-cell biology, although they support the involvement of Sin3A in instructing a mTORC1 signature possibly critical to Th17 differentiation.

Thus, we next investigated the expression of IL-17A, the signature cytokine for Th17 cells. We found that while a fraction of control cells expressed IL-17A after PMA and Ionomycin stimulation (PI), TAM-treated Sin3A-deficient cells mostly failed to do so (Fig 4A). At difference, cells produced IFN γ to comparable extents (Fig 4B). Defective IL-17A could not be attributed to differences in proliferation, as it was observed among Sin3A-sufficient and -deficient cells having undergone similar rounds of cell division (Appendix Fig S8A–C). Of note, a fraction of Sin3A-deficient cells preserved IL-17A expression (Appendix Fig S8D). RT-PCR analysis pointed toward a transcriptional defect, as Sin3A Δ cells revealed lower *Il17a* RNA levels compared with controls (Fig 4C), while *Ifng* levels were similar (Fig 4C and D). In addition to *Il17a*, also the expression of *Il17f*, *Il23r*, and *Il22* was lower in Sin3A-deleted cells. By contrast, *Il21* was significantly increased when compared to controls (Fig 4D). Thus, post-thymic genetic inactivation of Sin3A hinders proper differentiation of Th17 cells.

STAT3 and Foxp3 are upregulated in Sin3A-deficient CD4⁺ T cells in Th17-skewing conditions

Differentiation of Th17 helper cells depends on signals from IL-6, in combination with TGF- β , IL-23, and IL-21. These signals lead to the activation of STAT3 and the expression of ROR γ t, the Th17 lineage defining transcription factor. ROR γ t then acts in synergy with STAT3 (Ciofani et al, 2012), to promote the production of IL-17A, IL-17F, and IL-22 (Ivanov et al, 2006; Zhou et al, 2007; Manel et al, 2008) (Fig 5A).

As Sin3A controls STAT3 transcriptional activity in several cell types (Icardi et al, 2012; Gambi et al, 2019), we first investigated relative STAT3 expression, phosphorylation, and nuclear representation. We found a trend toward increased levels of total STAT3 and of its phosphorylation on Ser727 in cells lacking Sin3A compared with controls (Fig 5B and C). In addition, nuclear STAT3 levels were significantly higher in Sin3A-deficient cells than in controls (Fig 5D and E). This is in line with the transcriptomic data suggesting an upregulation of mTORC1 (Fig 3) that is upstream of STAT3, and suggest that in cells lacking Sin3A STAT3 might be more transcriptionally active.

Next, we analyzed ROR γ t expression. Data indicated ROR γ t to be expressed at comparable levels in Th17 skewed Sin3A-sufficient and -deficient cells both at the protein (Fig 5F–H) and mRNA level (Fig 5I). Thus, cells lacking Sin3A preserve the expression of STAT3 and ROR γ t. However, while *Il21*, which mainly relies on STAT3 (Wei et al, 2007), was expressed at higher levels in cells lacking Sin3A (Fig 4D), *Il17a*, *Il23r*, and *Il22*, which are concomitantly regulated by STAT3 and ROR γ t (Ivanov et al, 2006; Durant et al, 2011; Ciofani et al, 2012), failed to be properly induced. These data support the notion that STAT3 and not ROR γ t are transcriptional active in Th17 cells lacking Sin3A.

STAT3 also controls Foxp3 expression (Pallandre et al, 2007). In turns, Foxp3 can directly interact with ROR γ t, and inhibit *Il17a*

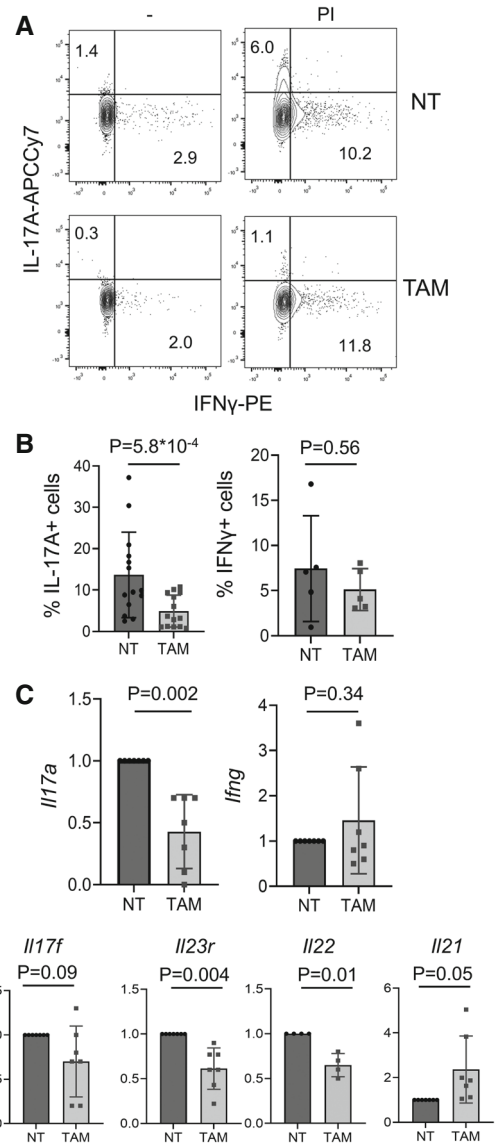


Figure 4. Sin3A-deficient T cells fail to differentiate in Th17 skewing conditions.

Sin3A^{F/F} Rosa26-CreER^{T2} CD4 T cells treated or not with TAM were kept for 3 days in Th17-skewing conditions as described in Fig 2. Cells were then left untreated or stimulated with PMA/ionomycin (PI) for 4 h, and analyzed by intracellular cytokine staining (A, B) or RT-PCR (C, D).

A, B (A) Representative dot plots and (B) bar plots showing the percentage of cells expressing IL-17A⁺ (N = 14) and IFN γ ⁺ (N = 5).

C, D RT-PCR analysis of indicated gene expression after PI stimulation. Relative levels are depicted: *Il17a*, *ifng*, *Il17f*, *Il21* (N = 7), *Il22* (N = 4), *Il23r* levels were analyzed without re-stimulation (N = 7).

Data information: In (B–D) data are presented as mean (Bars) \pm SD. Two-tailed paired Student’s t-test. N = 14, 5, or 7 cultures per condition (NT or TAM) derived from individual mice, as indicated.

transcription (Ichiyama et al, 2008; Zhou et al, 2008). We thus asked whether the absence of Sin3A could favor the expression of Foxp3 in spite of Th17 skewing conditions, and whether this might account for defective of *Il17a* upregulation. Cells lacking Sin3A were

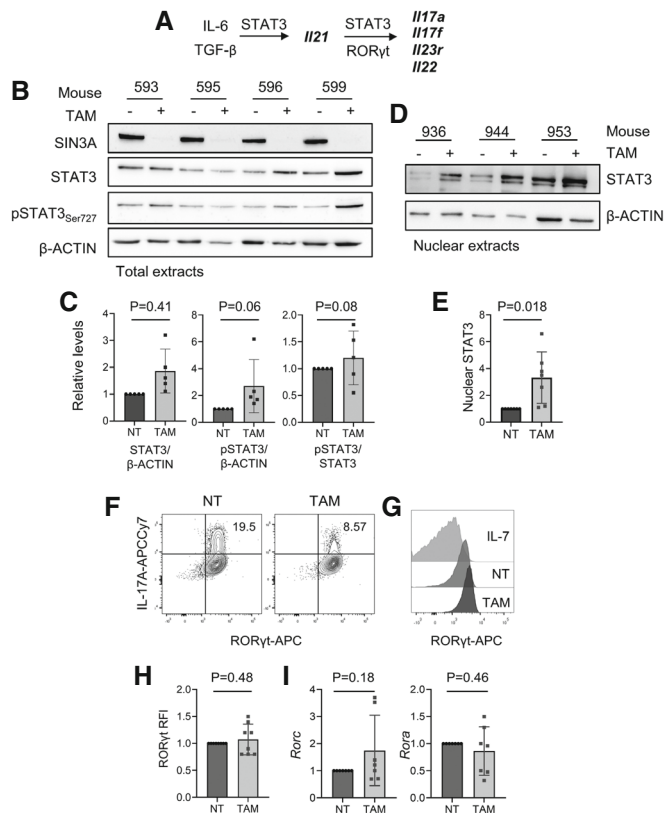


Figure 5. STAT3 and ROR γ t are properly expressed in Sin3A-deficient cells and yet fail to promote IL17A.

- A** Schematic representation of STAT3 and ROR γ t-driven events over Th17 differentiation.
- B–E** Representative western blot of total (B) and nuclear (D) STAT3 and pSTAT3 (ser727) in control (NT) and Sin3A-deleted Th17-skewed CD4⁺ T cells (TAM), and quantification of relative representation over independent experiments (C–E). Data relative to Sin3A and actin is also depicted in Fig 2E, as part of the same source file.
- F** Contour plots depicting IL-17A and ROR γ t levels in viable PMA and Ionomycin stimulated control (NT) and TAM-treated CD4⁺ T cells.
- G, H** (G) Representative histograms of ROR γ t protein levels and (H) relative expression (Relative Fluorescence Intensity, TAM relative to NT), $N = 8$.
- I** RT-PCR analysis of *Rorc* ($N = 6$) and *Rora* ($N = 7$) gene levels. Relative expression is shown.

Data information: In (B and C) Western Blot. $N = 4$ and 3 mice. In (D, E, H, I) data are presented as mean (Bars) \pm SD. Statistical analyses: in (E, H, I) Two-tailed paired Student's *t*-test. $N = 5, 7, 8, 7$ cultures per condition (NT or TAM) derived from individual mice, as indicated. In D pSTAT3/ β -ACTIN: Wilcoxon matched-pairs signed rank test (not normally distributed according to Shapiro–Wilk test). Source data are available online for this figure.

indeed enriched for Foxp3⁺ cells (Fig 6A and B), in line with the upregulation of *Foxp3* mRNA levels (Fig 6C).

TAM is known to activate mTOR signaling and to increase the number of splenic Treg in mice. Furthermore, estrogen receptor signaling is known to affect Treg development/differentiation (Rich et al, 2002). To further verify whether TAM affected Th17 cell differentiation, we treated cultures of CD4⁺ T cells obtained from Cre⁺ F/+ (Sin3A sufficient, wild-type) or Cre⁺ F/F (Sin3A-deficient cells,

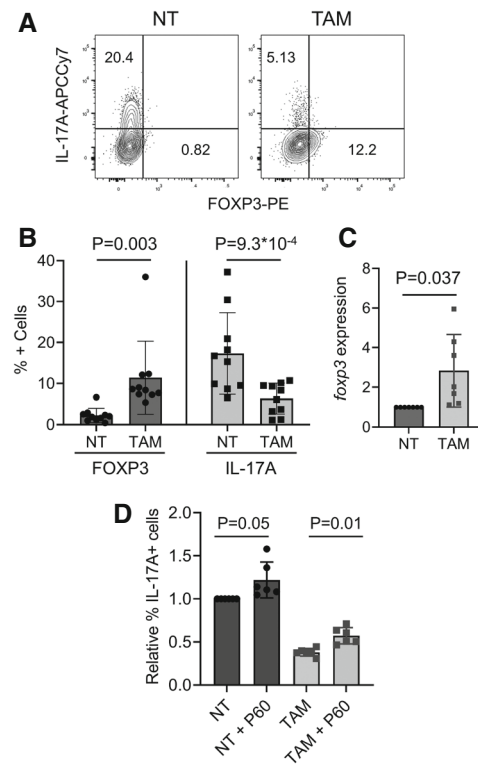


Figure 6. Sin3A inactivation favors the differentiation of Foxp3⁺ cells.

Cells were cultured as depicted in Fig 2 and analyzed after PMA and Ionomycin stimulation for 4 h.

- A, B** (A) Representative contour plots and (B) percentages of IL-17A⁺ and Foxp3⁺ cells, $N = 10$.
- C** RT-PCR analysis of *Foxp3* expression $N = 7$.
- D** Cells were cultured as depicted in Fig 2 in the absence or the presence of the P60 Foxp3 inhibitor. Cells were then harvested and stimulated with PMA and Ionomycin for 4 h. Bar plots report the percentage of IL-17A⁺ cells relative to untreated controls, $N = 6$.

Data information: In (B–D) data are presented as mean (Bars) \pm SD. Two-tailed paired Student's *t*-test. $N = 10, 7$ or 6 cultures per condition (NT or TAM) derived from individual mice, as indicated.

knockout) mice. Data indicate that TAM had no effect on IL-17, IL-2, IFN- γ , or Foxp3 (Appendix Fig S9A–D).

We noted that Foxp3 and IL-17A proteins were mutually exclusive (Fig 6A). We thus asked whether interfering with FoxP3 activity would rescue IL-17A expression. To this aim, we took advantage of P60, a cell permeable 15-mer synthetic peptide reported to bind to Foxp3 and to prevent its nuclear translocation (Casares et al, 2010). Sin3A-sufficient and -deficient cells were cultured in Th17 skewing conditions in the absence or the presence of P60, and then analyzed for IL-17A expression. We found that adding the P60 inhibitor over the course of Th17 differentiation significantly increased the percentage of IL-17A⁺ cells (Fig 6D), with no effects on cell viability (Appendix Fig S10A). Although the rescue was more statistically relevant for Sin3A-deficient cells, both Sin3A-sufficient and -deficient cells had increased percentage of IL-17A⁺ cells (Fig 6D). Thus, although a higher fraction of Sin3A-deficient cells acquires Foxp3 expression, this does not fully explain reduced IL-17A levels.

IL-2 contributes to the establishment of IL-17A⁺ Foxp3⁺ phenotype in Th17 skewed Sin3A-deficient cells

IL-2 promotes mTORC1 signaling (Ray et al, 2015), STAT3, and STAT5 phosphorylation and activation and Foxp3 expression and stability (Setoguchi et al, 2005; Zorn et al, 2006; Chen et al, 2011). As Sin3A was previously reported to negatively regulate *Il2* transcription by bringing HDAC to its promoter (Lam et al, 2015b), we reasoned that the loss of Sin3A could unleash increased IL-2 expression, and this could contribute to the upregulation of FoxP3 and defective *Il17a* expression. By FACS analysis, we found that Sin3A-deficient cultures were indeed enriched in IL-2-producing cells (Fig 7A and B), which was corroborated by higher *Il2* mRNA levels (Fig 7C), and a rise in phosphorylated STAT5, and p70S6 kinase (Appendix Fig S11A–D). These data provide a mechanistic explanation for the finding that Sin3A-deficient cells were characterized by the mTORC1 signaling signature. Thus, Sin3A inactivation unleash *Il2* transcription in Th17 conditions, and this might cause *Il17a*/IL-17A inhibition.

To directly challenge the role of IL-2, we investigated whether neutralizing IL-2 during Th17 skewing would impact on relative expression of FoxP3 and IL-17A. FACS analyses indicated that the addition of anti-IL-2 neutralizing antibodies had minimal effects on Sin3A-sufficient cultures, while it lowered the frequency of Foxp3⁺ cells almost to significant levels in Sin3A-deficient cultures. Concomitantly, neutralizing IL-2 increased the frequency of IL-17A⁺ cells only in cells lacking Sin3A, while had no effects on Sin3A-sufficient controls (Fig 7D and E). Notably, the rescue in IL-17A⁺ cells was proportional to the dose of anti-IL-2 Ab (Fig 7F), independent of cell viability (Appendix Fig S10B), and inversely correlated with the frequency of IL-2⁺ cells (Fig 7G). Thus, inactivation of Sin3A favors IL-2 upregulation, which neutralization partially rescues IL-17A⁺ cells, and limits Foxp3.

To better understand the relationship of IL-2, IL-17, and Foxp3, a logistic model was adopted for the unsupervised classification of samples based on their relative expression of these molecules. The scatter plots depicted in Appendix Fig S12A indicate that samples were assigned to independent categories (TAM-treated and untreated) with 95% confidence only when IL-2 versus IL-17A or Foxp3 versus IL-17A were considered. Instead, when IL-2 and Foxp3 were analyzed, Sin3A-sufficient (untreated) and -deficient (TAM treated) clustered together. Thus, together these data indicate that IL-2-producing cells are more likely to express Foxp3 rather than IL-17A.

RORγt accumulates in the cytoplasm in Sin3A-deficient T cells

IL-2 neutralization partially restored IL-17⁺ cells, and yet did not fully overcome the failure of Sin3A-deficient T cells to express IL-17A. Proteomics studies have identified several phosphorylation, acetylation, and ubiquitination sites in RORγt controlling nuclear localization, protein stability, DNA-binding, and transcriptional activity. In addition, previous reports indicated that cytoplasm-to-nuclear import is controlled by the PI3K-mTOR axis over the course of differentiation (Kurebayashi et al, 2012). Given the notion that Sin3A can interact with acetylases and deacetylases including p300 and Sirtuin1, both able to control RORγt acetylation (Lim et al, 2015; Wu et al, 2015), and that genes implicated in mTORC1

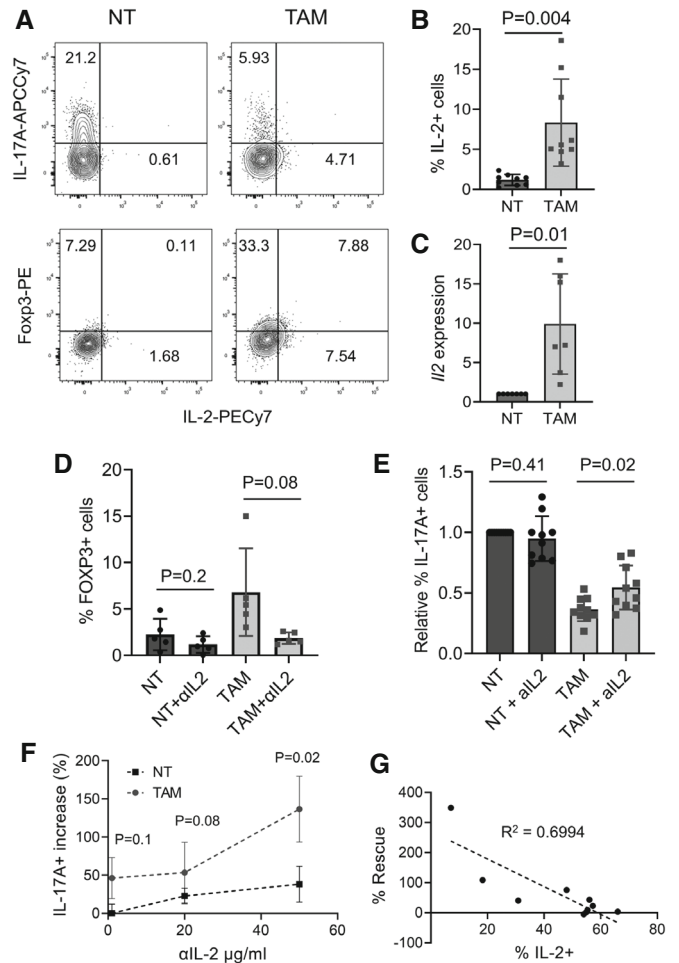


Figure 7. Sin3A-sensitive IL-2 upregulation limits the differentiation of IL-17A⁺ T cells.

- A, B Cells were cultured as depicted in Fig 2 and then stimulated with PMA and Ionomycin for 4 h. A. Representative contour plots and B. percentages of IL-2⁺ cells, N = 7.
- C RT-PCR analysis of *Il2* expression, N = 7.
- D, E Cells were cultured as depicted in Fig 2 in the absence or the presence of a neutralizing anti-IL-2 mAb. D. Bar plot depicting the frequency of Foxp3⁺, N = 5 and E. relative IL-17A⁺ cells, N = 10.
- F Relative increase in IL-17A⁺ Sin3A-sufficient and -deficient cells with respect to the dose of anti-IL-2 mAb, N = 3.
- G Correlation of the relative increase in IL-17A⁺ cells in the presence of anti-IL-2 antibody and the percentage of IL-2⁺ cells in TAM-treated cells.

Data information: In (B–E) data are presented as mean (Bars) ± SD. Two-tailed paired Student’s t-test. N = 9, 7, 5, 10 cultures per condition (NT or TAM) derived from individual mice, as indicated. In (F) each dot represents the mean ± SD of three independent determinations. Two-tailed paired Student’s t-test.

signaling pathway are upregulated upon Sin3A inactivation (Fig 3F–H), we asked whether RORγt could be regulated posttranscriptionally by Sin3A. To this aim, we analyzed RORγt subcellular distribution by confocal immunofluorescence analyses. While RORγt was detected in the nucleus of the vast majority of Sin3A-sufficient cells, a consistent fraction of Sin3A-deficient ones showed cytoplasmic relocalization of RORγt (Fig 8A), resulting in a consistent fraction of

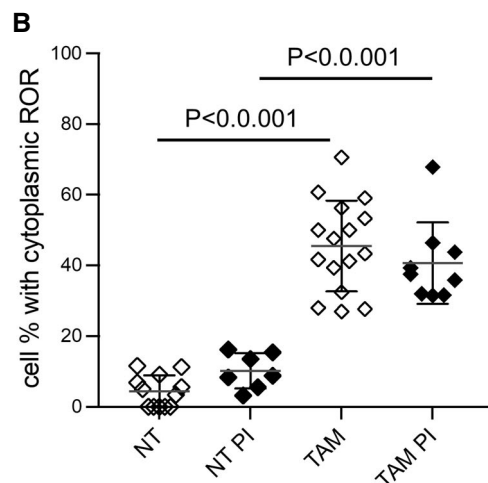
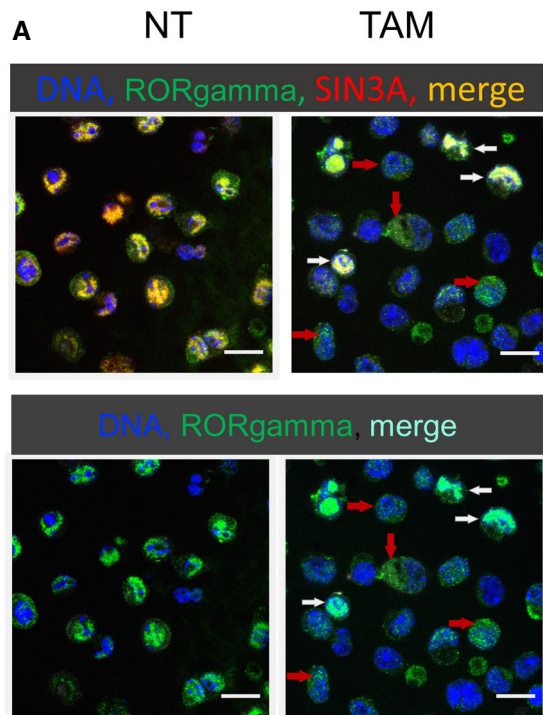


Figure 8. ROR γ t accumulates in the cytoplasm of Sin3A-deficient T cells.

Cells were cultured as depicted in Fig 2 and then left untreated or stimulated with PMA and Ionomycin for 4 h. Cells were then deposited on Poly-L-lysine coated coverslips, fixed, permeabilized and stained with anti-ROR γ t and anti-Sin3A antibodies. Nuclei were stained with Hoechst 33342.

A Representative confocal images are depicted. Scale bars: 10 μ m. Red and gray arrows indicate representative Sin3A-deficient and -sufficient cells, respectively.

B Plots depict the fraction of cells with cytoplasmic ROR γ t.

Data information: In (B), Dots represent individual images with 20–50 cells, collected over two independent experiments. An average of 300 cells was counter per conditions. Cells with picnotic nuclei or with vacuolated cytoplasm were excluded. Statistical analysis: One way Anova.

the cells with reduced nuclear ROR γ t representation (Fig 8A and B). Thus, cells lacking Sin3A show delocalization of ROR γ t, likely contributing to defective expression of *Il17a*, *Il23r*, and *Il22*.

Taken together, our data identify a previously unappreciated role for Sin3A in Th17 differentiation (schematically depicted in Appendix Fig S12B). Results support its ability to control IL-2, mTOR, STAT3, and ROR γ t ultimately shaping the immunoregulatory phenotype of T cells over the course of Th17 differentiation.

Discussion

The transcriptional regulator Sin3A controls several pathways governing many aspects of normal and neoplastic growth and survival. Here, we provide further evidence that Sin3A is absolutely required for CD4⁺ thymocyte development, and uncover its critical role in mature CD4⁺ T-cell survival and differentiation into Th17 effector cells.

In a previous study, Cowley *et al* (2005) reported that Lck-Cre-driven deletion of Sin3A at the DN3 stage of thymocyte development resulted in the arrest of CD8 immature precursors, and only allowed the maturation of dysfunctional CD4SP cells. By adopting CD4-Cre and CD4-CreER^{T2} deleter strains, we found that also inactivation of Sin3A past the DN stage, and more precisely at the DP stage severely halted both CD4⁺ and CD8⁺ thymocyte maturation, causing peripheral T-cell lymphopenia. In Sin3A-CD4 Δ mice, the large majority of remaining CD4⁺ T cells in secondary lymphoid organs had escaped Sin3A deletion. Thus, deletion of Sin3A in the thymus, either at the DN (Cowley *et al*, 2005) or at the DP stage (this manuscript), is not compatible with mature CD4 T-cell development and survival. In peripheral blood and secondary lymphoid organs of Sin3A-CD4 Δ , we found cells that had escaped deletion and acquired a memory phenotype. By contrast, Sin3A-deficient ones remained naïve. Based on unpublished data, we predict those cells to die shortly after TCR cross-linking. Of note, also CD25⁺Foxp3 CD4⁺ T cells did not accumulate upon Sin3A deletion. This further strengthens its role in survival.

The reasons accounting for the different impact of Sin3A deletion, that is, at the DN (Cowley *et al*, 2005) or DP (shown here), according to the timing of Sin3A deletion remain to be fully clarified. However, it should be noted that while DN thymocytes undergo a rapid and extensive proliferative phase (6–8 cell cycle division) to ensure the generation of a large pool of progenitors, DP cells enter a resting phase to allow rearrangement of the TCR alpha chain (Taghon *et al*, 2006; Ciofani & Zúñiga-Pflücker, 2007). Indeed, by performing single cell RNA-seq analyses, Li *et al* (2021) found that up to 40% of intermediate SP were in the M/G1 phase, while this was not the case for DP blasts. Thus, it could be speculated that deletion of Sin3A at the DN stage (Cowley *et al*, 2005) results in the selection of a cell subset capable to survive positive thymic selection, and yet lacking proper responsiveness at the mature stage. By contrast, inactivation of Sin3A at the DP stage, beyond TCR rearrangement, might render developing precursors more sensitive to negative selection. This is supported by the finding that Sin3A-deficient thymocytes were enriched for apoptotic cells. A role for ROR γ t

might also be envisaged. Indeed, it normally enforces a resting state in developing thymocytes and favors their survival via Bcl-XL upregulation (Sun *et al*, 2000). Given the finding that upon Sin3A deletion in mature T cells, ROR γ t accumulates in the cytoplasm, and direct ROR γ t targets are defectively induced, it is possible that ROR γ t functions are also altered in Sin3A-deficient thymocytes. Ongoing experiments are addressing this aspect. Inactivation of Sin3A in mature CD4 T cells showed that T cells failed to persist, strengthening the role of Sin3A in controlling survival.

To analyze the role of Sin3A in mature T cells, we adopted TAM-induced *in vitro* deletion. We found that post-thymic Sin3A inactivation was compatible with cell proliferation and their differentiation into memory cells. Although a slight enrichment of apoptotic cells and of cells arrested in the S-phase in cultures was detected within Sin3A-deficient cells, previously reported in other model systems by us and others (Dannenberg *et al*, 2005; McDonel *et al*, 2012; Gambi *et al*, 2019), Sin3A-sufficient and -deficient (TAM-treated) cells completed comparable rounds of cell division and acquired several memory markers. By Day 3, Sin3A knockdown cells also revealed a distinct mTORC1 signaling signature, corroborated by higher CD25 and PD-1 surface levels, and increased phosphorylation of p70S6K, an mTORC1 effector molecule (Brunn *et al*, 1996). Nevertheless, in Th17 skewing conditions, Sin3A-deficient cells failed to produce IL-17A because of *Il17a* defective expression. Compared with controls, Sin3A-deficient T cells also failed to upregulate *Il17f*, *Il23*, and *Il22*, typical determinants of Th17 cell differentiation, and instead upregulated *Il21* to higher extents when compared to controls. As *Il21* is more dependent on STAT3 (Wei *et al*, 2007), while *Il17a*, *Il23R*, and *Il22* require ROR γ t (Zhou *et al*, 2007), these data are consistent with STAT3 (increased phosphorylation and nuclear representation), and not ROR γ t being transcriptionally active.

Cells lacking Sin3A also upregulated *Il2* and were enriched for IL-2⁺ cells. Lam *et al* (2015b) previously found that Sin3A represses *Il2* expression by bringing histone deacetylase (HDAC) activity to *Il2* promoter regions. The binding of Sin3A/HDAC was relieved by TCR/Cdk5-induced Sin3A phosphorylation, which promoted IL-2 expression (Lam *et al*, 2015b). Our Sin3A-deficient T cells might lack this inhibitory mechanism. Augmented IL-2 played an active role. Indeed, neutralizing anti-IL-2 antibodies significantly increased IL-17A⁺ cells in Sin3A-deficient cultures, and concomitantly lowered the frequency of Foxp3⁺ cells, although not to statistical significance.

Foxp3 expression in human and mouse T cells is mediated by STAT3, which is activated downstream to CD3/CD28 and TGF β signaling (Pallandre *et al*, 2007). Foxp3 stability is also controlled by IL-2 (Chen *et al*, 2011). In Sin3A-deficient T cells, STAT3 appeared transcriptionally active, when considering *Il21*. In spite of previous reports highlighting the ability of active STAT3 to inhibit Foxp3, we found it to be upregulated. Specific phosphorylation of STAT3 at Serine 727 was shown to be induced by IL-6 via Cdk5 and needed for Foxp3 inhibition (Lam *et al*, 2015a). We speculate that in steady-state conditions, Sin3A restrains STAT3 downstream to IL-6. Interestingly, in Sin3A-deficient T cells, we found increased total and pSTAT3_{Ser727} levels. Given that Sin3A can bind Cdk5 (Lam *et al*, 2015b), it would be tempting to speculate that the loss of Sin3A might lower pSTAT3_{Ser727} representation within Foxp3 enhancer regions, thus allowing Foxp3 expression. To further elucidate this, the characterization of putative differences in STAT3 promoter occupancy in Sin3A-deficient cells compared with controls

and of the nature of the regulatory complexes possible affected by Sin3A deficiency would need to be investigated.

Thus, our data suggest that in Th17 conditions, Sin3A normally restrains IL-2 and Foxp3 expression. We initially hypothesized that the acquisition of Foxp3 might account for ROR γ t malfunctioning. Indeed, Zhou *et al* (2008) reported that TGF β -induced Foxp3 inhibits ROR γ t through direct interaction (Zhou *et al*, 2008). In this study, ROR γ t and Foxp3 were found co-expressed in naive CD4⁺ T cells exposed to TGF- β , and Foxp3-mediated inhibition of ROR γ t was relieved by IL-6, IL-21, and IL-23 promoting Th17 cell differentiation.

The finding that Foxp3 and IL-17A were mutually expressed and that the Foxp3 P60 inhibitor (Casares *et al*, 2010) partially rescued IL-17A⁺ cells supported this notion. However, P60 also increased IL-17⁺ cells in control cultures, suggesting that Foxp3 and Sin3A act via independent mechanisms, and that additional mechanisms might contribute to defective *Il17a* expression.

Accordingly, we found that T cells lacking Sin3A had increased ROR γ t representation in the cytoplasm compared with controls. This could directly explain reduced expression of target genes. The nuclear localization of ROR γ t is regulated by import into the nucleus, and export from the nucleus. The former is controlled by PI3K-Akt-mTORC1-dependent signals (Limagne *et al*, 2017). Once into the nucleus, ROR γ t phosphorylation and acetylation modulate ROR γ t activity. For instance, phosphorylation via the extracellular signal regulated kinases (ERKs) restrict Th17 activity (Ma *et al*, 2022). The effects of acetylation/deacetylation by histone acetyltransferases and histone acetyldeacetylases on ROR γ t function have been studied with somehow contradictory conclusions. Lim *et al* (2015) reported that ROR γ t acetylation impaired DNA-binding and hence transcriptional activity. In line with this notion, naive CD4⁺ T cells transduced with K69/81/99Q mutants mimicking a constitutively acetylated form of ROR γ t, failed to differentiate into Th17 cells. By contrast, Wu *et al* (2015) found that p300 can acetylate ROR γ t at K81 residue and increase its stability, as well as transcriptional activity. The same authors found that HDAC1 counteracted p300 activity. The histone deacetylase Sirtuin 1 (SIRT1) has also been shown to deacetylate ROR γ t and by that promote Th17 differentiation (Lim *et al*, 2015). Of note, STAT3 acetylation affects its ability to translocate into the nucleus (Zhuang, 2013). STAT3 can heterodimerize with either the histone deacetylase SIRT1 or the histone acetylase p300. Limagne and co-authors reported that SIRT1 agonists blunted STAT3 acetylation and caused its retention in the cytoplasm. These authors also found that, SIRT1 did not interact with STAT3 but with ROR γ t in Th17 cells in the absence of SIRT1 activation. Upon activation, SIRT1 did no longer interact with ROR γ t, but instead with STAT3, causing its cytoplasmic retention (Limagne *et al*, 2017). Sin3A can form complexes with both p300 and HDAC1 (Kadamb *et al*, 2013; Dancy & Cole, 2015; Tsai *et al*, 2017). Future studies will have to determine whether these Sin3A complexes can bind ROR γ t and if so, which could be the acetylation status of ROR γ t in Sin3A-sufficient and -deficient cells, and how this would impact on its subcellular distribution.

Together, our data indicate that Sin3A regulates IL-2, mTOR, STAT3, Foxp3, and ROR γ t over the course of Th17 differentiation balancing immunoregulatory phenotypes. Whether similar events also shape Th17 cell function *in vivo* remains to be determined. Indeed, our attempts to trace mature T cells upon Sin3A inactivation failed, as

CD4⁺ Sin3A deleted cells lacked *in vivo* persistence. Nevertheless, a subset of T cells within the small intestinal lamina propria was found to co-express both Foxp3 and ROR γ t and to produce less IL-17 than those that express ROR γ t alone (Zhou *et al*, 2008), suggesting that Th17 cells can acquire distinct physiological functions in response to extracellular signals (cytokines/growth factors). We suggest that Sin3A contributes to such differentiation program, by directly or indirectly tuning IL-2, mTORC1, STAT3, Foxp3, and ROR γ t. Although some controversy regarding the role of mTORC1 signaling on Foxp3 expression exists (Battaglia *et al*, 2005; Kopf *et al*, 2007), it has been shown to regulate the generation and function of central and effector Foxp3⁺ regulatory T cells (Sun *et al*, 2018). It is thus tempting to suggest that IL-2 and/or agents directly tuning mTORC1 (i.e., nutrients, microbial components) (McGeachy & McSorley, 2012) might shape the inflammatory/regulatory phenotype of Th17 cells. As Sin3A inhibitors have been developed for *in vivo* use, these data also raise the possibility to target Sin3A (Kwon *et al*, 2015) in autoimmune diseases or gut inflammatory disorders. In these conditions, Sin3A inhibition could dampen the pro-inflammatory nature of Th17 cells, while favoring immunoregulatory functions.

Materials and Methods

Mice

Mice were housed and bred in the San Raffaele Institutional specific pathogen-free animal facilities. Mice used in this study were backcrossed with C57BL/6J mice (> 10 generations). Mice carrying Sin3A-floxed alleles (Dannenberget *et al*, 2005) (Sin3A^{F/F}; gently provided by Dr. Jan Tavernier, Ghent University and Hospital, Ghent University, 9000 Ghent, Belgium) were crossed with CD4-Cre (Lee *et al*, 2001) (gently provided by Dr. Paolo Dellabona, San Raffaele Institute), CD4-CreER^{T2} (gently provided by Burkhard Becher, University of Zurich), or Rosa26-CreER^{T2} (Ventura *et al*, 2007) (gently provided by Dr. Marco Bianchi, San Raffaele Institute) transgenic mice to generate Sin3A^{F/F} CD4-Cre^{+/-}, Sin3A^{F/F} CD4-CreER^{T2} ^{+/-} and Sin3A^{F/F} Rosa26-CreER^{T2} ^{+/-} mice, respectively. Sin3A^{F/F} mice were also crossed with OT II mice (gently provided by Dr. Andrea Annoni, San Raffaele Institute) and subsequently with Rosa26-CreER^{T2} ^{+/-} mice. Mice were screened by PCR. The following primers were used to detect the floxed (250 bp) or wild-type (150 bp) Sin3A allele: 5'-CAGATCCTATTCCAGGTGTC AAAG and 5'-CATGTTTCATGTTAGATATACTTCG. The presence (390 bp) of Cre was also investigated by PCR with the following primers 5'-CCTGAAAATGCTTCTGTCCG and 5'-CAGGGTGTATAAGCAATCCC. Studies were performed in accordance with the European Union guidelines and with the approval of the San Raffaele Institute Institutional Ethical Committee (Milan, Italy; IACUC-814).

T cell activation and differentiation

CD4⁺ T cells were isolated by negative selection from spleens and lymph nodes (Miltenyi Biotec, #130-104-454) according to the manufacturer's instructions (typically > 95% purity). To initiate Sin3A deletion, CD4⁺ T cells were then cultured for 6 days in RPMI supplemented with 5% FBS, L-Glutamine, Pen/Strep, β -mercaptoethanol and IL-7 (5 ng/ml) in the absence or the presence of 4-OH tamoxifen (TAM, 1 μ M). Cells (1 \times 10⁶/ml) were then recovered and activated

for 3 days on plate-bound anti-CD3 (BD, #553058) and soluble anti-CD28 (Biolegend, #102116) antibodies in the indicated skewing conditions, in the absence or the presence of TAM (0.5 μ M). For Th17 differentiation, T cells were plated on 5 μ g/ml plate-bound anti-CD3 and 5 μ g/ml anti-CD28 antibodies in Iscove's Modified Dulbecco's Medium (IMDM) supplemented with 10% FBS, L-Glutamine, Pen/Strep, β -mercaptoethanol, 50 ng/ml IL-6, 1 ng/ml TGF- β , 10 ng/ml IL-1 β , 10 μ g/ml anti-IL-4 and 10 μ g/ml anti-IFN γ . For Th0 differentiation, T cells were cultured on 1 μ g/ml plate-bound anti-CD3 and 1 μ g/ml soluble anti-CD28 antibodies in RPMI supplemented with 5% FBS, L-Glutamine, Pen/Strep, β -mercaptoethanol, 20 ng/ml IL-2 and 2.3 ng/ml TGF- β . For Th1 differentiation, cells were cultured as in Th0, supplementing cells with 3 μ g/ml anti-IL-4 and 10 ng/ml IL-12. For Treg differentiation, T cells were cultured on 1 μ g/ml plate-bound anti-CD3 and 5 μ g/ml soluble anti-CD28 antibodies in RPMI supplemented with 5% FBS, L-Glutamine, Pen/Strep, β -mercaptoethanol, 20 ng/ml IL-2 and 2.3 ng/ml TGF- β . All cytokines used were purchased from Peprotech. After 3 days of activation, cells were stimulated with Phorbol 12-myristate 13-acetate (PMA) (10 ng/ml, Sigma, #P8139)/ionomycin (1 μ g/ml, Sigma, #I0634) for 4 h, adding Brefeldin A (BFA) (5 μ g/ml, sigma, #B7651) for the last 2 h of culture. As control, half of the cells were treated only with BFA. In some experiments, anti-IL-2 blocking antibody (1 μ g/ml unless specified, BioCell #BE0043-1) or the Foxp3 inhibitor P60 (Casares *et al*, 2010) (20 μ M) were provided during the 3 days Th17 differentiating cultures.

In experiments using OTII^{+/-} Sin3A CreERT2 mice, CD4 T cells were purified as above, kept for 6 days in RPMI supplemented with 5% FBS, L-Glutamine, Pen/Strep, β -mercaptoethanol and IL-7 (5 ng/ml) in the absence or the presence of 4-OH tamoxifen (TAM, 1 μ M) and then cultured for 3 days in Th17 conditions in the presence of 1.25 μ M ovalbumin (OVA).

Flow cytometry

Cells were collected, washed in PBS, and stained with a viable dye (Zombie Aqua, Biolegend, #423101) for 20 min on ice in the dark. Cells were then resuspended in Fc-blocking solution (anti CD16/CD32 antibody 2.4G2, homemade), incubated for 5 min and then labeled with indicated antibodies for 15 min at 4°C in the dark. Cells were then washed and fixed for 30 min to ON at 4°C (Foxp3/Transcription Staining Buffer Set, eBioscience, #00-5523-00). Fixed cells were permeabilized using the same buffer set and intracellular stainings were performed for 30 min at 4°C in the dark. Stained cells were collected and measured on a BD FACSCanto3 machine. Analyses were performed using the FlowJo software. The list of antibodies adopted in the study is provided in Appendix Table S1.

Apoptosis and cell proliferation

To measure apoptosis, surface levels of Annexin V were investigated by flow cytometry. 1 \times 10⁵ cells were washed and resuspended in 100 μ l of ice-cold binding buffer (140 mM NaCl, 4 mM KCl, 0.75 mM MgCl2 and 10 mM HEPES). Ten minutes before acquisition, anti-AnnexinV-FITC antibody (5 μ l, BD, #51-65874X), 7-AAD (5 μ l, BD, #559925) and 1.75 μ l of 85 mM CaCl₂ were added. Proliferation was determined by labeling T cells with the Tag-IT Violet Proliferation Cell Tracking Dye (Biolegend, #425101), according to the manufacturer

instructions. Briefly, cells were washed twice with PBS, resuspended in PBS (100×10^6 cell/ml), and incubated with Tag-It Violet Proliferation Cell Tracking Dye ($5 \mu\text{M}$) for 20-min RT in the dark. Then, an equal volume of FBS was added to the sample, and cells were finally washed with and 10 ml cell culture medium.

Cell cycle analysis

CD4^+ T cells (1×10^6) were washed twice with cold PBS, resuspended in 500 μl PBS, fixed by adding 4.5 ml ice-cold 70% ethanol while vortexing and incubated for at least 2 h at 4°C . Samples were centrifuged, washed with PBS for 15 min RT, incubated in 300 μl of 1 $\mu\text{g}/\text{ml}$ DAPI 0.1% Triton X-100 in PBS for 30 min and acquired in linear mode at low speed.

RNA-Seq analysis

Illumina strand-specific mRNA Roughly 100 ng of high-quality total RNA ($\text{RIN} > 8$) was used for the transcriptomic interrogation of control and SIN3A deleted CD4 T cells using Illumina's Stranded mRNA Prep ligation according to the manufacturer's instructions. Briefly, Oligo(dT) magnetic beads were used to purify and capture the mRNA molecules in the total RNA. The purified mRNA was fragmented and copied into first strand complementary DNA (cDNA) using reverse transcriptase and random primers. A second strand cDNA synthesis step removed the RNA template while incorporating dUTP in place of dTTP in order to preserve strand specificity. Next, double-stranded cDNA was A-tailed, then ligated to Illumina anchors bearing T-overhangs. PCR-amplification of the library allowed the barcoding of the samples with 10 bp dual indexes and the completion of Illumina sequences for cluster generation. Libraries were quantified with Qubit dsDNA HS Assay Kit and their profile was examined using Agilent's HS D1000 ScreenTape Assay. Sequencing was carried out in an Illumina NextSeq2000 using paired end, dual-index sequencing (Rd1: 59 cycles; i7: 10 cycles; i5: 10 cycles, Rd2 59 cycles) at a depth of 30 million reads per sample.

RNA-seq reads are trimmed using Trim Galore v0.4.4 using default parameters to remove the Nextera adapter sequence. Mapping is performed using STAR (2.6) against the mouse NCBI37 genome, guided by gene models from Ensembl annotation release 68. Quantification and generation of gene expression matrices were performed with the function featureCounts, implemented in the R package Rsubread. Aligned fragments are imported into RStudio and before statistical analysis, the function filterbyExpr, implemented in the R package edgeR, was used to determine genes with enough counts for further analyses. Differential gene expression analysis is performed using the DESeq2 algorithm within R and RStudio. Gene set enrichment analysis was carried out using GSEA software (<https://www.gsea-msigdb.org/>).

RT-PCR and real-time PCR

Total RNA was purified using ReliaPrep RNA Miniprep System (Promega, #Z6011), according to the manufacturer's instructions. RNA was retrotranscribed for 1 h at 42°C with retro transcriptase M-MLV (Invitrogen, #28025-013) in the presence of oligo(dT)₁₅ Primer (Promega, #C1101), dNTPs (Euroclone), and RNasin Ribonuclease Inhibitor (Promega, #N2111). The cDNA was diluted 10 times to

perform qRT-PCR with SYBR Green Master Mix (Applied Biosystems, #4309155). The list of primers adopted in the study is provided in Appendix Table S2. C_t values were normalized to the housekeeping gene UbiquitinC by the $\Delta\Delta C_t$ method.

Western blot

Total lysates were recovered in 2% SDS Tris-HCl 65 mmol/l pH 6.8 lysis buffer and sonicated. Whole cell, cytosolic, and nuclear extracts were obtained using the REAP protocol (Suzuki et al, 2010). Lysates corresponding to the same number of cells were separated by SDS-PAGE, transferred to nitrocellulose membrane, blocked with phosphate buffered solution (PBS)-5% milk, and subjected to immunoblotting. In some cases, membranes were stripped using a mild stripping buffer (15 g/l glycine, 1 g/l SDS, 1% Tween 20, pH 2.2). A protein size marker was loaded on the gels as reference (Amersham ECL Rainbow Marker full range, GERPN800E, Merck). The following antibodies were used: Anti-STAT3 (Cell Signaling, #9139), anti-(Ser727) STAT3 (Cell Signaling, #9134), anti- β -ACTIN (Cell Signaling, #3700), and anti-SIN3A (Cell Signaling, #7691). Quantification of protein levels was performed by measuring the mean gray value of the bands using ImageJ.

Confocal immunofluorescence analyses

T cells were cultured in Th17 conditions and treated or not with PMA and Ionomycin for 4 h. Cells were then deposited on Poly-L-lysine coated coverslips in duplicates, fixed for 10 min at RT with 3.7% Paraformaldehyde in PHEM buffer (60 mM PIPES, 25 mM HEPES, 10 mM EGTA, 4 mM MgSO_4) and permeabilized with ice-cold Sucrose-HEPES-Triton-X100 buffer, for 5 min on ice. Coverslips were washed, blocked in 4% BSA, 10% Normal Goat Serum and eventually incubated with primary antibodies (1:200) for 1–2 h at RT. Anti-ROR gamma (t) (AFKJS-9), eBioscience, #14-6988-82 and anti-Sin3A (Abcam #129087) were validated and used. After washing, coverslips were incubated with Alexa-labeled secondary antibodies (1 $\mu\text{g}/\text{ml}$, Abcam), nuclei stained with Hoechst 33342, and images were sequentially acquired with a $63\times 1.4\text{NA}$ objectives using Leica TCS SP5 confocal microscope equipped with 405, 488, 546, and 633 nm lasers obtaining images at 1024×1024 pixel resolution with 16-bit pixel depth. Images were acquired and analyzed using ImageJ (Schindelin et al, 2009), and data processed in Excel. Plots and statistical analyses were performed with Prism software.

Statistical analyses

Unless otherwise indicated, a paired two-tailed Student's *t*-test was used. *P*-values < 0.05 were considered significant. Error bars represents standard deviations (SD). GraphPad Prism 9 was used to perform statistical analyses.

Logistic model

A logistic model was adopted to assign the distribution of TAM-treated or untreated cells based on selected markers. The R stats package (version 4.0.2) for logistic model fitting and the R ggplot2 package (version 3.3.3) were used and run in Rstudio (version 1.0.153).

Data availability

The datasets and computer code produced in this study are available in the following databases: RNA-Seq data: Gene Expression Omnibus GSE196615 (<https://www.ncbi.nlm.nih.gov/geo/query/acc.cgi?acc=GSE196615>).

Expanded View for this article is available [online](#).

Acknowledgements

Laura Icardi was supported by fellowships funded by the San Raffaele International Postdoctoral Programme (INVEST) and the Associazione Italiana per la Ricerca sul Cancro (AIRC-iCare) with partial financial support by the European Commission (FP7–Marie Curie Actions–People– COFUND). Gobierno de Navarra Industria (0011-1411-2022-000088, SOCRATHeS), Ministerio de Ciencia e Innovación (PLEC2021-008094 MCIN/AEI/10.13039/501100011033) (granted to JLL). Instituto de Salud Carlos III (ISCIII) and co-financed by FEDER: CIBERONC CB16/12/00489 (granted to FP). The authors are grateful to Dr. Jan Tavernier (Ghent University) for the provision of Sin3A^{FF} mice, Dr. Paolo Dellabona (San Raffaele Institute) for the provision of CD4-Cre mice, and Dr. Marco Bianchi (San Raffaele Institute) for the provision of Rosa26-ER^{T2}Cre mice. Finally, the authors would like to thank Dr. Maya Fedeli (San Raffaele Institute) for help with thymic analysis and for anti-IL-2 antibodies, Dr. Christopher Bruhn (FIRC Institute of Molecular Oncology, IFOM, Milan, Italy) for help with the logistic models and present and past members of the Mondino's lab for frequent discussion. Open access funding provided by BIBLIOSAN.

Author contributions

Laura Perucho: Conceptualization; data curation; formal analysis; investigation. **Laura Icardi:** Conceptualization; data curation; methodology. **Elisabetta Di Simone:** Formal analysis; investigation; methodology. **Veronica Basso:** Data curation; formal analysis; investigation; methodology. **Alessandra Agresti:** Data curation; formal analysis. **Amaia Vilas Zornoza:** Methodology. **Teresa Lozano:** Data curation; formal analysis. **Felipe Prosper:** Resources; formal analysis; methodology. **Juan José Lasarte:** Data curation; formal analysis; supervision. **Anna Mondino:** Conceptualization; data curation; formal analysis; supervision; funding acquisition; writing – original draft; writing – review and editing.

Disclosure and competing interests statement

The authors declare that they have no conflict of interest.

References

- Alland A, Muhle R, Hou H Jr, Potes J, Chin L, Schreiber-Angus N, DePinho RA (1997) Role for N-CoR and histone deacetylase in Sin3-mediated transcriptional repression. *Nature* 387: 49–55
- Ayer DE, Lawrence QA, Eisenman RN (1995) Mad-max transcriptional repression is mediated by ternary complex formation with mammalian homologs of yeast repressor Sin3. *Cell* 80: 767–776
- Battaglia M, Stabilini A, Roncarolo MG (2005) Rapamycin selectively expands CD4⁺CD25⁺FoxP3⁺ regulatory T cells. *Blood* 105: 4743–4748
- Brunn GJ, Williams J, Sabers C, Wiederrecht G, Lawrence JC, Abraham RT (1996) Direct inhibition of the signaling functions of the mammalian target of rapamycin by the phosphoinositide 3-kinase inhibitors, wortmannin and LY294002. *EMBO J* 15: 5256–5267
- Casares N, Rudilla F, Arribillaga L, Llopiz D, Riezu-Boj JI, Lozano T, López-Sagaseta J, Gumbre L, Sarobe P, Prieto J et al (2010) A peptide inhibitor of FOXP3 impairs regulatory T cell activity and improves vaccine efficacy in mice. *J Immunol* 185: 5150–5159
- Chaubal A, Pile LA (2018) Same agent, different messages: insight into transcriptional regulation by SIN3 isoforms. *Epigenetics Chromatin* 11: 1–11
- Chen Q, Kim YC, Laurence A, Punkosdy GA, Shevach EM (2011) IL-2 controls the stability of Foxp3 expression in TGF-β-induced Foxp3⁺ T cells *in vivo*. *J Immunol* 186: 6329–6337
- Ciofani M, Zúñiga-Pflücker JC (2007) The thymus as an inductive site for T lymphopoiesis. *Annu Rev Cell Dev Biol* 23: 463–493
- Ciofani M, Madar A, Galan C, Sellars M, Mace K, Pauli F, Agarwal A, Huang W, Parkurst CN, Muratet M et al (2012) A validated regulatory network for Th17 cell specification. *Cell* 151: 289–303
- Cowley SM, Iritani BM, Mendrysa SM, Xu T, Cheng PF, Yada J, Liggitt HD, Eisenman RN (2005) The mSin3A chromatin-modifying complex is essential for embryogenesis and T-cell development. *Mol Cell Biol* 25: 6990–7004
- Dancy BM, Cole PA (2015) Protein lysine acetylation by p300/CBP. *Chem Rev* 115: 2419–2452
- Dannenberg J, David G, Zhong S, Van Der Torre J, Wong WH, Depinho RA (2005) mSin3A corepressor regulates diverse transcriptional networks governing normal and neoplastic growth and survival. *Genes Dev* 19: 1581–1595
- Das J, Ren G, Zhang L, Roberts AI, Zhao X, Bothwell ALM, Van Kaer L, Shi Y, Das G (2009) Transforming growth factor β is dispensable for the molecular orchestration of Th17 cell differentiation. *J Exp Med* 206: 2407–2416
- Dong C (2008) TH17 cells in development: an updated view of their molecular identity and genetic programming. *Nat Rev Immunol* 8: 337–348
- Durant L, Watford WT, Ramos HL, Laurence A, Vahedi G, Takahashi H, Sun H, Kanno Y, Powrie F, Shea JJO (2011) Diverse targets of the transcription factor STAT3 contribute to T cell pathogenicity and homeostasis. *Immunity* 32: 605–615
- Fazio TG, Huff JT, Panning B (2008) An RNAi screen of chromatin proteins identifies Tip60-p400 as a regulator of embryonic stem cell identity. *Cell* 134: 162–174
- Gambi G, Di Simone E, Basso V, Ricci L, Wang R, Verma A, Elemento O, Ponzoni M, Inghirami G, Icardi L et al (2019) The transcriptional regulator Sin3A contributes to the oncogenic potential of STAT3. *Cancer Res* 79: 3076–3087
- Heideman MR, Lancini C, Proost N, Yanover E, Jacobs H, Dannenberg JH (2014) Sin3a-associated Hdac1 and Hdac2 are essential for hematopoietic stem cell homeostasis and contribute differentially to hematopoiesis. *Haematologica* 99: 1292–1303
- Icardi L, Mori R, Gesellchen V, Eyckerman S, De Cauwer L, Verhelst J, Vercauteren K, Saelens X, Meuleman P, Leroux-Roels G et al (2012) The Sin3a repressor complex is a master regulator of STAT transcriptional activity. *Proc Natl Acad Sci USA* 109: 12058–12063
- Ichiyama K, Yoshida H, Wakabayashi Y, Chinen T, Saeki K, Nakaya M, Takaesu G, Hori S, Yoshimura A, Kobayashi T (2008) Foxp3 inhibits RORγt-mediated IL-17A mRNA transcription through direct interaction with RORγt. *J Biol Chem* 283: 17003–17008
- Ivanov II, McKenzie BS, Zhou L, Tadokoro CE, Lepelley A, Lafaille JJ, Cua DJ, Littman DR (2006) The orphan nuclear receptor RORγt directs the differentiation program of proinflammatory IL-17⁺ T helper cells. *Cell* 126: 1121–1133

- Jiang Y, Wang X, Dong C (2019) *Molecular mechanisms of T helper 17 cell differentiation: emerging roles for transcription cofactors*, 1st edn. London: Elsevier Inc
- Kadamb R, Mittal S, Bansal N, Batra H, Saluja D (2013) Sin3: insight into its transcription regulatory functions. *Eur J Cell Biol* 92: 237–246
- Kopf H, de la Rosa GM, Howard OMZ, Chen X (2007) Rapamycin inhibits differentiation of Th17 cells and promotes generation of FoxP3⁺ T regulatory cells. *Int Immunopharmacol* 7: 1819–1824
- Korn T, Bettelli E, Gao W, Awasthi A, Jäger A, Strom TB, Oukka M, Kuchroo VK (2007) IL-21 initiates an alternative pathway to induce proinflammatory T H17 cells. *Nature* 448: 484–487
- Korn T, Bettelli E, Oukka M, Kuchroo VK (2009) IL-17 and Th17 cells. *Annu Rev Immunol* 27: 485–517
- Kurebayashi Y, Nagai S, Ikejiri A, Ohtani M, Ichiyama K, Baba Y, Yamada T, Egami S, Hoshii T, Hirao A et al (2012) PI3K-Akt-mTORC1-S6K1/2 axis controls Th17 differentiation by regulating Gfi1 expression and nuclear translocation of ROR γ . *Cell Rep* 1: 360–373
- Kwon Y-J, Petrie K, Leibovitch BA, Zeng L, Mezei M, Howell L, Gil V, Christova R, Bansal N, Yang S et al (2015) Selective inhibition of SIN3 corepressor with avermectins as a novel therapeutic strategy in triple negative breast cancer. *Mol Cancer Ther* 14: 1824–1836
- Lachmann A, Xu H, Krishnan J, Berger SI, Mazloom AR, Maayan A (2010) ChEA: transcription factor regulation inferred from integrating genome-wide CHIP-X experiments. *Bioinformatics* 26: 2438–2444
- Laherty CD, Yang WM, Jian-Min S, Davie JR, Seto E, Eisenman RN (1997) Histone deacetylases associated with the mSin3 corepressor mediate Mad transcriptional repression. *Cell* 89: 349–356
- Lam E, Choi SH, Pareek TK, Kim BG, Letterio JJ (2015a) Cyclin-dependent kinase 5 represses Foxp3 gene expression and Treg development through specific phosphorylation of Stat3 at Serine 727. *Mol Immunol* 67: 317–324
- Lam E, Pareek TK, Letterio JJ (2015b) Cdk5 controls IL-2 gene expression via repression of the mSin3a-HDAC complex. *Cell Cycle* 14: 1327–1336
- Lee PP, Fitzpatrick DR, Beard C, Jessup HK, Lehar S, Makar KW, Pérez-Melgosa M, Sweetser MT, Schlissel MS, Nguyen S et al (2001) A critical role for Dnmt1 and DNA methylation in T cell development, function, and survival. *Immunity* 15: 763–774
- Li Y, Li K, Zhu L, Li B, Zong D, Cai P, Jiang C, Du P, Lin J, Qu K (2021) Development of double-positive thymocytes at single-cell resolution. *Genome Med* 13: 1–18
- Liang SC, Tan XY, Luxenberg DP, Karim R, Dunussi-Joannopoulos K, Collins M, Fouser LA (2006) Interleukin (IL)-22 and IL-17 are coexpressed by Th17 cells and cooperatively enhance expression of antimicrobial peptides. *J Exp Med* 203: 2271–2279
- Lim HW, Kang SG, Ryu JK, Schilling B, Fei M, Lee IS, Kehasse A, Shirakawa K, Yokoyama M, Schnölzer M et al (2015) SIRT1 deacetylates ROR γ t and enhances Th17 cell generation. *J Exp Med* 212: 607–617
- Limagne E, Thibaudin M, Euvrard R, Berger H, Chalons P, Végan F, Humblin E, Boidot R, Rébé C, Derangère V et al (2017) Sirtuin-1 activation controls tumor growth by impeding Th17 differentiation via STAT3 deacetylation. *Cell Rep* 19: 746–759
- Loonstra A, Vooijs M, Beverloo HB, Al Allak B, van Drunen E, Kanaar R, Berns A, Jonkers J (2001) Growth inhibition and DNA damage induced by Cre recombinase in mammalian cells. *Proc Natl Acad Sci USA* 98: 9209–9214
- Ma S, Patel SA, Abe Y, Chen N, Patel PR, Cho BS, Abbasi N, Zeng S, Schnabl B, Chang JT et al (2022) ROR γ t phosphorylation protects against T cell-mediated inflammation. *Cell Rep* 38: 110520
- Manel N, Unutmaz D, Littman DR (2008) The differentiation of human TH-17 cells requires transforming growth factor- β and induction of the nuclear receptor ROR γ t. *Nat Immunol* 9: 641–649
- Mathur AN, Chang H-C, Zisoulis DG, Stritesky GL, Yu Q, O'Malley JT, Kapur R, Levy DE, Kansas GS, Kaplan MH (2007) Stat3 and Stat4 direct development of IL-17-secreting Th cells. *J Immunol* 178: 4901–4907
- McDonel P, Demmers J, Tan DWM, Watt F, Hendrich BD (2012) Sin3a is essential for the genome integrity and viability of pluripotent cells. *Dev Biol* 363: 62–73
- McGeachy MJ, McSorley SJ (2012) Microbial-induced Th17: superhero or supervillain? *J Immunol* 189: 3285–3291
- Nagai S, Kurebayashi Y, Koyasu S (2013) Role of PI3K/Akt and mTOR complexes in Th17 cell differentiation. *Ann NY Acad Sci* 1280: 30–34
- Nagy L, Kao HY, Chakravarti D, Lin RJ, Hassig CA, Ayer DE, Schreiber SL, Evans RM (1997) Nuclear receptor repression mediated by a complex containing SMRT, mSin3A, and histone deacetylase. *Cell* 89: 373–380
- Nakamura T, Mori T, Tada S, Krajewski W, Rozovskaia T, Wassell R, Dubois G, Mazo A, Croce CM, Canaani E (2002) ALL-1 is a histone methyltransferase that assembles a supercomplex of proteins involved in transcriptional regulation. *Mol Cell* 10: 1119–1128
- Pal S, Yun R, Datta A, Lacomis L, Erdjument-Bromage H, Kumar J, Tempst P, Sif S (2003) mSin3A/histone deacetylase 2- and PRMT5-containing Brg1 complex is involved in transcriptional repression of the Myc target gene cad. *Mol Cell Biol* 23: 7475–7487
- Pallandre J-R, Brillard E, Créhange G, Radlovic A, Remy-Martin J-P, Saas P, Rohrlich P-S, Pivot X, Ling X, Tiberghien P et al (2007) Role of STAT3 in CD4⁺CD25⁺FOXP3⁺ regulatory lymphocyte generation: implications in graft-versus-host disease and antitumor immunity. *J Immunol* 179: 7593–7604
- Ray JP, Staron MM, Shyer JA, Ho PC, Marshall HD, Gray SM, Laidlaw BJ, Araki K, Ahmed R, Kaech SM et al (2015) The Interleukin-2-mTORc1 kinase axis defines the signaling, differentiation, and metabolism of T helper 1 and follicular B helper T cells. *Immunity* 43: 690–702
- Rich RL, Hoth LR, Geoghegan KF, Brown TA, Lemotte PK, Simons SP, Hensley P, Myszka DG (2002) Kinetic analysis of estrogen receptor/ligand interactions. *Proc Natl Acad Sci USA* 99: 8562–8567
- Rincon M, Pereira FV (2018) A new perspective: mitochondrial stat3 as a regulator for lymphocyte function. *Int J Mol Sci* 19: 1656
- Schindelin J, Arganda-Carrera I, Frise E, Verena K, Mark L, Tobias P, Stephan P, Curtis R, Stephan S, Benjamin S et al (2009) Fiji - an open platform for biological image analysis. *Nat Methods* 9: 676–682
- Schreiber-Agus N, Chin L, Chen K, Torres R, Rao G, Guida P, Skoultschi AI, DePinho RA (1995) An amino-terminal domain of Mxi1 mediates anti-myc oncogenic activity and interacts with a homolog of the yeast transcriptional repressor SIN3. *Cell* 80: 777–786
- Skisel GD, Mirsoian A, Minnar CM, Crittenden M, Curti B, Chen JQ, Blazar BR, Borowsky AD, Monjazeb AM, Murphy WJ (2017) Differential phenotypes of memory CD4 and CD8 T cells in the spleen and peripheral tissues following immunostimulatory therapy. *J Immunother Cancer* 5: 1–11
- Setoguchi R, Hori S, Takahashi T, Sakaguchi S (2005) Homeostatic maintenance of natural Foxp3⁺CD25⁺CD4⁺ regulatory T cells by interleukin (IL)-2 and induction of autoimmune disease by IL-2 neutralization. *J Exp Med* 201: 723–735
- Sun Z, Unutmaz D, Zou YR, Sunshine MJ, Pierani A, Brenner-Morton S, Mebius RE, Littman DR (2000) Requirement for ROR γ in thymocyte survival and lymphoid organ development. *Science* 288: 2369–2373
- Sun I-H, Oh M-H, Zhao L, Patel CH, Arwood ML, Xu W, Tam AJ, Blosser RL, Wen J, Powell JD (2018) mTOR complex 1 signaling regulates the

- generation and function of central and effector Foxp3⁺ regulatory T cells. *J Immunol* 201: 481–492
- Suzuki K, Bose P, Leong-Quong RY, Fujita DJ, Riabowol K (2010) REAP: a two minute cell fractionation method. *BMC Res Notes* 3: 294
- Taghon T, Yui MA, Pant R, Diamond RA, Rothenberg EV (2006) Developmental and molecular characterization of emerging β - and $\gamma\delta$ -selected pre-T cells in the adult mouse thymus. *Immunity* 24: 53–64
- Tan JT, Dudl E, LeRoy E, Murray R, Sprent J, Weinberg KI, Surh CD (2001) IL-7 is critical for homeostatic proliferation and survival of naïve T cells. *Proc Natl Acad Sci USA* 98: 8732–8737
- Tsai WB, Long Y, Chang JT, Savaraj N, Feun LG, Jung M, Chen HHW, Kuo MT (2017) Chromatin remodeling system p300-HDAC2-Sin3A is involved in arginine starvation-induced HIF-1 α degradation at the ASS1 promoter for ASS1 derepression. *Sci Rep* 7: 1–12
- Ventura A, Kirsch DG, McLaughlin ME, Tuveson DA, Grimm J, Lintault L, Newman J, Reczek EE, Weissleder R, Jacks T (2007) Restoration of p53 function leads to tumour regression *in vivo*. *Nature* 445: 661–665
- Wei L, Laurence A, Elias KM, O'Shea JJ (2007) IL-21 is produced by Th17 cells and drives IL-17 production in a STAT3-dependent manner. *J Biol Chem* 282: 34605–34610
- Wu Q, Nie J, Gao Y, Xu P, Sun Q, Yang J, Han L, Chen Z, Wang X, Lv L et al (2015) Reciprocal regulation of ROR γ t acetylation and function by p300 and HDAC1. *Sci Rep* 5: 1–11
- Yang X, Zhang F, Kudlow JE (2002) Recruitment of O-GlcNAc transferase to promoters by corepressor mSin3A: coupling protein O-GlcNAcylation to transcriptional repression. *Cell* 110: 69–80
- Yang XO, Panopoulos AD, Nurieva R, Seon HC, Wang D, Watowich SS, Dong C (2007) STAT3 regulates cytokine-mediated generation of inflammatory helper T cells. *J Biol Chem* 282: 9358–9363
- Yang R, Lirussi D, Thornton TM, Jelley-Gibbs DM, Diehl SA, Case LK, Madesh M, Taatjes DJ, Teuscher C, Haynes L et al (2015) Mitochondrial Ca²⁺ and membrane potential, an alternative pathway for interleukin 6 to regulate CD4 cell effector function. *Elife* 4: 1–22
- Ye P, Rodriguez FH, Kanaly S, Stocking KL, Schurr J, Schwarzenberger P, Oliver P, Huang W, Zhang P, Zhang J et al (2001) Requirement of interleukin 17 receptor signaling for lung CXC chemokine and granulocyte colony-stimulating factor expression, neutrophil recruitment, and host defense. *J Exp Med* 194: 519–527
- Yosef N, Shalek AK, Gaublotte JT, Jin H, Lee Y, Awasthi A, Wu C, Karwacz K, Xiao S, Jorgolli M et al (2013) Dynamic regulatory network controlling TH17 cell differentiation. *Nature* 496: 461–468
- Zhou L, Ivanov II, Spolski R, Min R, Shenderov K, Egawa T, Levy DE, Leonard WJ, Littman DR (2007) IL-6 programs TH-17 cell differentiation by promoting sequential engagement of the IL-21 and IL-23 pathways. *Nat Immunol* 8: 967–974
- Zhou L, Lopes JE, Chong MMW, Ivanov II, Min R, Victora GD, Shen Y, Du J, Rubtsov YP, Rudensky AY et al (2008) TGF- β -induced Foxp3 inhibits TH17 cell differentiation by antagonizing ROR γ t function. *Nature* 453: 236–240
- Zhuang S (2013) Regulation of STAT signaling by acetylation. *Physiol Behav* 25: 1924–1931
- Zorn E, Nelson EA, Mohseni M, Porcheray F, Kim H, Litsa D, Bellucci R, Raderschall E, Canning C, Soiffer RJ et al (2006) IL-2 regulates FOXP3 expression in human CD4⁺CD25⁺ regulatory T cells through a STAT-dependent mechanism and induces the expansion of these cells *in vivo*. *Blood* 108: 1571–1579



License: This is an open access article under the terms of the [Creative Commons Attribution-NonCommercial-NoDerivs](https://creativecommons.org/licenses/by-nc-nd/4.0/) License, which permits use and distribution in any medium, provided the original work is properly cited, the use is non-commercial and no modifications or adaptations are made.